PHYSICAL REVIEW B VOLUME 14, NUMBER 8 15 OCTOBER 1976

Theory of vibrational mode intensities in inelastic electron tunneling spectroscopy*

John Kirtley,† D. J. Scalapino, and P. K. Hansma
Department of Physics, University of California, Santa Barbara, California 93106
(Received 2 February 1976)

We use a transfer-Hamiltonian formalism to develop a theory for the intensity of vibrational modes in inelastic electron tunneling spectroscopy (IETS) of organic molecules in metal-insulator-metal junctions. The initial and final electron states are localized on opposite sides of the insulating barrier and are described by Wentzel-Kramers-Brillouin (WKB) wave functions. The interaction potential between the tunneling electron and the vibrating molecule is a sum of Coulomb potentials; each element in the sum corresponding to a partial charge localized on an atom in the molecule. The theory predicts properly the magnitudes of the integrated intensities in IETS as well as the ratio of intensities for opposite bias voltages. It also predicts that Raman-active modes should be comparable in intensity to infrared modes, even neglecting bond polarizabilities, and that modes forbidden to optical spectroscopies may be observable in IETS. We further describe how the orientation of the doped molecules on the surface can be inferred from IETS intensities.

I. INTRODUCTION

Inelastic electron tunneling spectroscopy (IETS) is a sensitive technique for measuring the vibrational spectra of organic molecules in monolayer and submonolayer coverages on solid surfaces.[1,2] Measurements are done on metal-oxide-doped impurity-metal tunneling junctions. The spectra obtained are the second derivatives of the current-voltage characteristics of these junctions: specifically, d^2V/dI^2 as a function of voltage V. These second-derivative curves show sharp peaks at voltages corresponding to the vibrational mode energies of the doped impurities. The peaks occur because of the opening up of inelastic tunneling channels in which the electrons start from a filled state in one metal electrode, lose energy in exciting a vibrational mode of the doped impurity, and finish with sufficient energy to find an unoccupied final state in the other metal electrode.

The vibrational-mode energies as measured by IETS can be used in the same way as in infrared and Raman spectroscopy: for identifying unknown compounds and for obtaining information on molecular structure. The energies measured by IETS can be directly compared to those measured by infrared and Raman spectroscopy because energy shifts due to the top metal electrode are generally small, especially for modes below ≈200 meV (1600 cm^{-1}).[3]

The vibrational-mode intensities as measured by IETS have not yet received much attention. In this paper we show that these intensities can be calculated and that they contain useful information on the orientation of the molecular adsorbate.

Soon after the initial work on IETS by Jaklevic and Lambe, Scalapino and Marcus[4] formulated a theory for the peak intensities by including the dipole potential of the molecule and its image in the barrier potential and calculating the excess tunneling current within the WKB approximation for infrared-active modes. Jaklevic and Lambe[1] extended this analysis to Raman-active modes by including molecular polarizabilities. Duke[5] described a transfer-Hamiltonian technique based on first-order perturbation theory to model the effect of inelastic impurity excitations in tunneling junctions. Gadzuk[6] applied this treatment to vibrational-mode-assisted tunneling using a one-dimensional interaction potential. Klein *et al.*[7] used the same general formalism to describe MgO phonon-assisted tunneling. A number of authors[8] have succeeded in formulating theories of tunneling that do not depend on the transfer-Hamiltonian technique and its associated approximations. These theories are complex, however, and no one has yet succeeded in including a tunneling electron-molecule interaction of sufficient generality to describe measured tunneling spectra of molecular vibrations. We believe that the transfer-Hamiltonian provides an adequate description of the physical situation of interest, and its relatively simpler mathematical form allows us to focus on the structure of the electron-molecule interaction. Specifically, we write the interaction potential as a sum of Coulomb potentials between the tunneling electron and the partial charges on each atom of the molecule. We then calculate the inelastic tunneling matrix element using WKB wave functions for the incoming and outgoing states. The scattering process is treated in three dimensions, and we show that the inclusion of off-axis scattering results in conclusions that are different not only quantitatively but also qualitatively from purely one-dimensional calculations. Since we are using the electron-molecule interaction as a first-order perturbation on WKB-approximation wave functions, we cannot take into account the

elastic distortion of the incoming and outgoing wave functions due to the molecular impurity. The relatively-long-range structure of the interaction decreases the importance of this distortion for the vibrational-mode couplings. For electronic excitations this would not be the case.

We use the theory to predict absolute intensities and the ratios of intensities for opposite bias voltages. We extend the theory to calculate intensities for complex molecules and explore the selection rules in this new spectroscopy. Finally, we compare the theoretical predictions to experiment and find good agreement.

II. THEORY

Consider the sample geometry indicated in Fig. 1. The two metal electrodes fill the half-spaces $z<0$, $z>l$. The insulating barrier is semi-infinite, occupying the space $0<z<l$. The doped organic molecule is located inside the insulating barrier a short distance from the lower metal film at position $\vec{r}=a\hat{z}+b\hat{x}+c\hat{y}$. The initial and final electron states are eigenfunctions of the zeroth-order Hamiltonian

$$\mathcal{H}=-(\hbar^2/2m)\nabla^2+U(\vec{r}) \tag{1}$$

and are localized in the half-spaces $z>l$, $z<0$, respectively. Outside the barrier the wave functions are standing plane waves. Inside the barrier they decay exponentially in the $\hat{z}$ direction while oscillating in the $\hat{x}$ and $\hat{y}$ directions. We assume for simplicity that the insulating barrier potential has the form

$$U(z)=\begin{cases} U, & 0<z<l\,, \\ 0, & \text{otherwise}. \end{cases} \tag{2}$$

In this case the initial and final states have standard WKB wave forms within the tunneling region given by[9]

$$\psi_i=\frac{1}{\sqrt{2}L^{3/2}}\frac{k_z^{1/2}}{|K_z|^{1/2}}e^{-|K_z|(l-z)}e^{i(k_x x+k_y y)}\,,$$
$$\psi_f=\frac{1}{\sqrt{2}L^{3/2}}\frac{k_z'^{1/2}}{|K_z'|^{1/2}}e^{-|K_z'|z}e^{i(k_x' x+k_y' y)}\,. \tag{3}$$

In this expression k_x, k_y, and k_z are the wave vectors in the $\hat{x}$, $\hat{y}$, and $\hat{z}$ directions; the electron wave functions have been normalized within a cube of side L, and the rate of exponential decay of the wave forms inside the barrier is given by

$$|K_z|=(2m/\hbar^2)^{1/2}(U-\hbar^2k_z^2/2m)^{1/2}\,.$$

Rather than taking a dipole approximation for the tunneling electron-molecular interaction, we assume that the charge distribution within the molecule can be broken up into partial charges, with each partial charge localized on a particular atom. The partial charges arise from an uneven sharing of the electrons involved in bonding and can be obtained from the dipole derivatives of infrared theory. The partial charge analysis allows us to describe the interaction at distances comparable to interatomic lengths, distances within which the dipole approximation breaks down.

The total tunneling electron-molecular interaction is given by

$$V(\vec{r})=\sum_j\frac{-e^2Z_j}{|\vec{r}-\vec{R}_j|}\,, \tag{4}$$

where Z_je and R_j are the partial charge and position, respectively, of the jth atom. In order to connect initial and final electronic states of different energies, we separate out the component of the total interaction potential which oscillates at the frequency of the vibrational mode of interest. Expanding the $\vec{R}_j$'s in the first harmonic approximation $\vec{R}_j=\vec{R}_j(0)+\delta\vec{R}_j$ we find

$$V_I(\vec{r})\cong\sum_j-e^2Z_j\delta\vec{R}_j\cdot\vec{\nabla}_j\left(\frac{1}{|\vec{r}-\vec{R}_j(0)|}\right). \tag{5}$$

If we take the images of the partial charges in the two metal films into account, the interaction becomes

$$V_I(\vec{r})=\sum_{n=-\infty}^{\infty}\sum_j\frac{-e^2Z_j\delta\vec{R}_j\cdot\vec{\nabla}_j}{\epsilon}\times\left(\frac{1}{|\vec{r}-\vec{R}_j-2nl\hat{z}|}-\frac{1}{|\vec{r}-\vec{R}_j-(2nl-2a_j)\hat{z}|}\right). \tag{6}$$

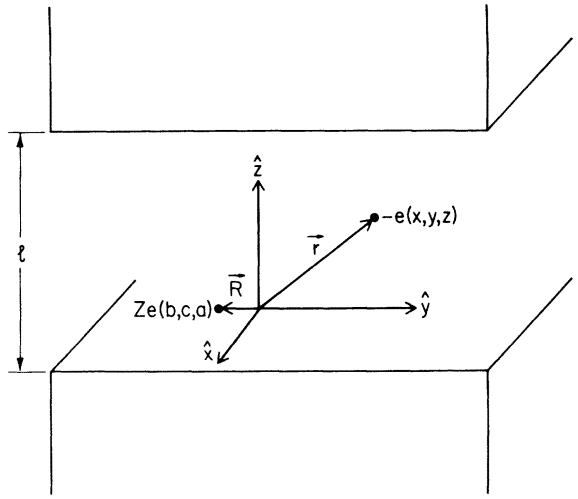

FIG. 1. Sample geometry and axes used in the theory presented in this paper. An oxide layer of width l is sandwiched in between two semi-infinite metal films in the half-planes $z<0$, $z>l$. A partial charge Ze lies within the barrier region at position $\vec{R}$ (b,c,a) close to the lower metal film and interacts with a tunneling electron at $\vec{r}$ (x,y,z).

In this expression the screening response of the insulating region has been approximated by a dielectric constant ϵ. Since the dielectric screening fields oscillate at the vibrational frequency, the proper ϵ to take is that for infrared frequencies. We assume that the metals are perfect conductors, since for the metals of interest at low temperatures and infrared frequencies $\epsilon_m \approx -400$.

There is some question as to where the image charges should be placed. Newns[10] calculates that the effective imaging plane is behind the atomic surface of the metal by λ^{-1}, where λ^{-1} is the Fermi-Thomas screening length. Lang and Kohn[11] in a somewhat more sophisticated model put the imaging plane in front of the atomic surface by roughly the same factor. A recent paper on the vibrational mode shifts in IETS due to the top metal electrode[3] attributed small but systematic downward shifts in the vibrational mode energies as compared with optical measurements to the interaction of the oscillating charges in the impurity molecules with their images in the metal surface. These shifts were fit to a simple image model using an adjustable charge to image plane distance on the order of 1 Å. The values for the atom to image plane distance obtained in this manner were used in the present work for calculating numerical results. Our results do not depend critically on this distance.

Fermi's golden rule for the transition rate from one electrode to the other is

$$w_{KK'} = (2\pi/\hbar)\,|M_{KK'}|^2 \delta(\epsilon_K - \epsilon'_K - \hbar\omega)\,. \tag{7}$$

The matrix element $M_{KK'}$ is defined as

$$M_{KK'} = \int_0^l d^3x\, \psi^*_{K'} V_I(\vec{r}, \omega t)\psi_K\,, \tag{8}$$

with $\psi_{K'}$ and ψ_K given by Eq. (3) and V_I given by Eq. (6).

The interaction potential falls rapidly to zero outside the tunneling region because of electronic screening at the metal surfaces. Therefore we need only integrate Eq. (8) over the oxide layer and can neglect the small component of the electronic wave function in the metal film opposite the film in which it is localized.

Consider a single atom of the molecule with partial charge Z_j oscillating around an equilibrium position $\vec{R}_j(0) = a\hat{z} + b\hat{x} + c\hat{y}$ with vector amplitude $\delta\vec{R}_j = \delta_j e^{i\omega t}\hat{j}$. The sum over atoms is done later. By Fourier transforming the interaction potential and summing a series of integrals in the complex q_z plane (where q_z is the Fourier conjugate to z), we find the following matrix element:

$$M_{KK'_j} = \frac{\pi e^2 Z_j \delta_j \zeta_z e^{-|K_z|l} e^{i\alpha_x b} e^{i\alpha_y c} \alpha_j}{\epsilon L^3 \alpha_\perp} \left[\frac{e^{\alpha_\perp a} \pm e^{-\alpha_\perp a}}{e^{2l\alpha_\perp} - 1} \left(\frac{e^{(\alpha_z - \alpha_\perp)l} - 1}{\alpha_\perp - \alpha_z} + \frac{e^{(\alpha_z + \alpha_\perp)l} - 1}{\alpha_\perp + \alpha_z} \right) \right.$$
$$\left. + \frac{1}{\alpha_\perp - \alpha_z} \left[e^{(\alpha_z - \alpha_\perp)l} (e^{\alpha_\perp a} \pm e^{-\alpha_\perp a}) - (e^{\alpha_z a} \pm e^{-\alpha_\perp a}) \right] + \frac{1}{\alpha_\perp + \alpha_z} (e^{\alpha_z a} - e^{-\alpha_\perp a}) \right], \tag{9}$$

where

$$\begin{aligned} \zeta_z &= k_z^{1/2} k_z'^{1/2} / |K_z|^{1/2} |K'_z|^{1/2}\,, \\ \alpha_x &= k_x - k'_x\,, \\ \alpha_y &= k_y - k'_y\,, \\ \alpha_z &= |K_z| - |K'_z|\,, \\ \alpha_\perp &= (\alpha_x^2 + \alpha_y^2)^{1/2}\,. \end{aligned} \tag{10}$$

The upper signs are taken and $\alpha_j = \alpha_\perp$ if $\hat{j} = \hat{z}$ (vibrations perpendicular to the metal surfaces). The lower signs are taken and $\alpha_j = \alpha_x, \alpha_y$ if $\hat{j} = \hat{x}$ or $\hat{y}$ (motion parallel to the metal surfaces).

To find the inelastic tunneling current we multiply the transition rate by $2e$ (2 for the spin sum) and sum over all initial and final wave vector states:

$$j = \frac{4\pi e}{\hbar} \sum_k \sum_{k'} |M_{KK'}|^2 f(\epsilon_K)[1 - f(\epsilon'_K + eV)] \times \delta(\epsilon_K - \epsilon_{K'} - \hbar\omega)\,. \tag{11}$$

Here ϵ_K and $\epsilon_{K'}$ are the total energies of the initial and final electronic states, V is the voltage bias of the junction, and $\hbar\omega$ is the energy spacing of the vibrational mode of interest. The Fermi distribution functions appear since electrons must tunnel from filled states to empty states.

In this formulation we assume implicitly that the vibrational mode has a δ-function response in frequency to the tunneling electron excitation. Real molecules have spectral weight distribution functions with nonzero bandwidths. However, the quantity to be compared with experiment is the change in conductance due to the onset of a given vibrational mode tunneling channel. This change in conductance is due to an integrated spectral weight over the band, and the shape of the distribution function is unimportant. If the shape of the lines were of interest, one would multiply Eq. (11) by the phonon spectral distribution function and integrate over energies. Experimentally observed lines are narrow, indicating weak coupling of the molecular modes to their surroundings.

The matrix element, Eq. (9), is in general a function of the incoming and outgoing energies and

directions. Using a standard spherical coordinate system we write

$$|M_{KK'}|^2 = \left| \sum_j M_{KK'_j} \right|^2 \equiv G(\epsilon, \epsilon', \Theta, \Theta', \varphi, \varphi') . \tag{12}$$

Further, since IETS spectra are normally taken at or below 4.2°K, we take the low-temperature limit $T \to 0$°K for the Fermi distribution functions. Changing the wave vector sum to an integral, we find

$$j = \frac{8\pi e}{\hbar}\left(\frac{L}{\pi}\right)^6\left(\frac{m}{\hbar^2}\right)^3 \int_0^{2\pi} d\varphi \int_0^{2\pi} d\varphi' \int_0^1 d(\cos\Theta) \int_0^1 d(\cos\Theta') \int_0^\infty \epsilon^{1/2} d\epsilon \int_0^\infty \epsilon'^{1/2} d\epsilon' \, G(\epsilon, \epsilon', \Theta, \Theta', \varphi, \varphi') \times [1 - \Theta(\epsilon - \epsilon_F)] \Theta(\epsilon' - \epsilon_F + eV) \delta(\epsilon - \epsilon' - \hbar\omega) , \tag{13}$$

where

$$\Theta(x) = 1, \quad x \geq 0; \quad \Theta(x) = 0, \quad x < 0 .$$

Evaluating Eq. (13) would be a formidable task, considering the complexity of the matrix elements. Fortunately, the quantity of experimental interest is the second derivative of Eq. (13) with respect to voltage. The step functions become δ functions upon differentiation, and the effect of the δ functions is to put the initial and final electron energies on the Fermi surface. This is just as one would expect; the onset of an inelastic tunneling channel occurs when the most energetic electrons find the first available open states as the voltage is increased. We obtain finally

$$\frac{d^2 j}{d(eV)^2} = \frac{8\pi e}{\hbar}\left(\frac{L}{\pi}\right)^6\left(\frac{m}{\hbar^2}\right)^3 (\epsilon_F)^{1/2}(\epsilon_F - eV)^{1/2} \int_0^{2\pi} d\varphi \int_0^{2\pi} d\varphi' \int_0^1 d(\cos\Theta) \int_0^1 d(\cos\Theta') G(\epsilon_F, \epsilon_F - eV, \Theta, \Theta', \varphi, \varphi') \delta(\hbar\omega - eV) . \tag{14}$$

In many cases the first azimuthal angular integration can be done analytically. The remaining integrations over incoming and outgoing angles are done numerically.

III. RESULTS AND DISCUSSION

A. Absolute intensities in IETS

We first compare the prediction for the absolute intensities in IETS with experiment. To find the change in conductance due to the opening of a vibrational-mode conduction path $[dj_i/d(eV)]$ we integrate Eq. (14) over energy across the vibrational band and multiply by n, the number of doping molecules per cm^2 on the oxide surface. (We assume that the surface of the oxide is uniformly covered with a given density n of noninteracting molecules per cm^2. If each molecule is vibrating independently of its neighbors, the individual contributions to the inelastic tunneling intensity merely add. If the molecules interact weakly with each other, then exact placement in the plane of the oxide surface is unimportant.) For a monolayer of hydroxyl ions (assumed oriented with their major axes in the $\hat{z}$ direction) we take $Z = 0.3$,[12] $\delta_{\text{rms}} = 0.07$ Å, $n = 10^{15}/\text{cm}^2$,[13] $\epsilon = 3$,[14] $\hbar\omega = 0.45$ eV, $l = 15$ Å, $a = 1$ Å, $U - \epsilon_F = 2$ eV. The choices of Z, δ, n, and ϵ are supported by infrared measurements, the value for $\hbar\omega$ is read directly from the tunneling spectrum, the choices of l and U are consistent with measurements of the I-V characteristics of the junctions, and the choice of a is consistent with measurements of frequency shifts in IETS due to the top metal electrode.[3,15] Using the above values, we find a predicted change in conductance:

$$\Delta \frac{dj_i}{d(eV)} = 3.9 \times 10^{20} \text{ A/J m}^2 . \tag{15}$$

A standard calculation for the elastic conductance using the same model and parameters for the barrier potential as above gives

$$\frac{dj_e}{d(eV)} = 7.0 \times 10^{22} \text{ A/J m}^2 . \tag{16}$$

Combining Eqs. (15) and (16) we find that the predicted change in the conductance due to the inelastic tunneling channel produced by a monolayer of O-H ions is $\approx \frac{1}{2}\%$. A typical experimental value is 0.4%.

B. Opposite voltage bias asymmetries of IETS intensities

A second test of the theory comes from measurements of the asymmetry of IETS intensities when junctions are biased in the two opposite polarities of voltage. Figure 2 shows plots of the second-harmonic voltage signal as a function of bias voltage for an Al–oxide–benzoic-acid–Pb sample. The upper curve is for Al negative with respect to the Pb, and the lower curve is for Al

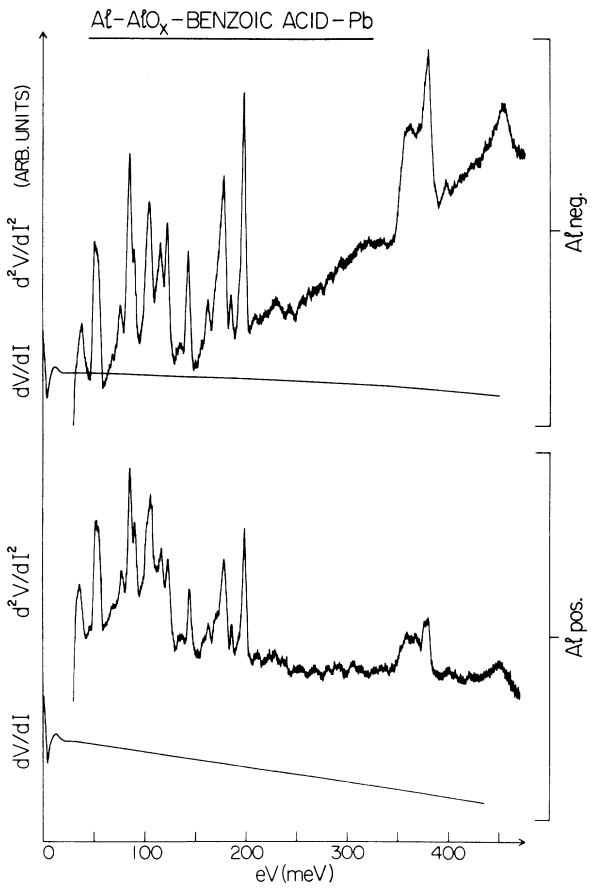

FIG. 2. Plots of the first and second derivatives (dV/dI and d^2V/dI^2) of an Al–Al_2O_3–benzoic-acid–Pb tunneling junction for Al biased negative (upper curves) and positive (lower curves). The IETS intensities are larger for Al biased negative. Note also the asymmetry in the dynamic resistance (dV/dI) curves.

positive with respect to the Pb. Also included are the first-harmonic voltage signals (proportional to the dynamic resistance of the junction) which show that the I-V characteristics of these junctions are asymmetric. (For example, the dynamic resistance dV/dI of the sample in Fig. 2 is 22% higher for aluminum biased negative than for aluminum biased positive at 300 meV.) All the curves were taken with a set current modulation resulting in a modulation voltage of ≈2 mV at 4.2°K. The inelastic electron tunneling response is larger when the electrons tunnel from the Al into the Pb than vice versa. We use the relation $d^2I/dV^2 = -g^3d^2V/dI^2$, where g is the dynamic conductance dI/dV, to plot the ratio of the integrated IETS intensities $\Delta[dj/d(eV)_+]/\Delta[dj/d(eV)_-]$ versus bias voltage in Fig. 3.

The physical reason for the asymmetry in inelastic tunneling intensities is that the doped molecules for the Al–oxide–benzoic-acid–Pb samples

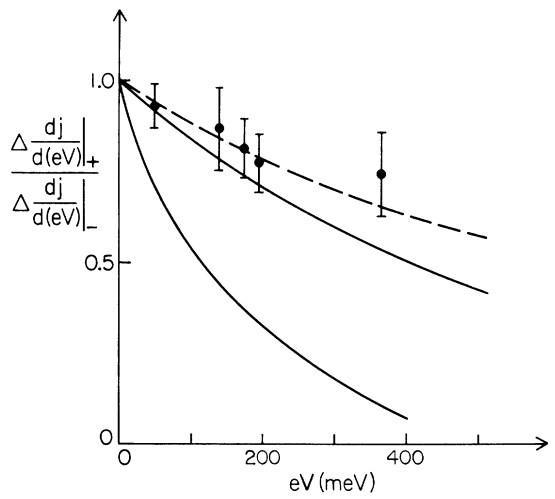

FIG. 3. Plot of the ratio of the IETS integrated intensities for Al positive divided by Al negative $\Delta[dj/d(eV)_+]/\Delta[dj/d(eV)_-]$ vs applied energy across the junction (in electron volts). The lower solid curve is based on a model proposed by Yanson *et al.* (Ref. 16). The upper solid curve is based upon the present theory for $l = 15$ Å, $U - \epsilon_F = 2$ eV, $a = 1$ Å. The dashed curve contains a small correction to the present theory for the elastic asymmetry of the junctions as described in the text.

are closest to the Pb-metal surface. When electrons tunnel from the Al to the Pb they cross more of the barrier before losing energy to a vibrational mode of the impurity than when they tunnel in the other direction. Thus, since electrons with higher energy are more likely to cross the barrier, we should expect greater inelastic tunneling intensities for Al negative with respect to Pb than vice versa.

This explanation for the bias asymmetries in IETS was offered first by Yanson *et al.*[16] They obtained the right sign for the effect, but (implicitly) assumed a very-short-range interaction and obtained predicted ratios for $\Delta[dj/d(eV)_+]/\Delta[dj/d(eV)_-]$ much smaller than observed experimentally. The lower curve in Fig. 3 is based on their model with $l = 15$ Å, $U - \epsilon_F = 2$ eV.

The present theory has a long-range dipole potential, and we would therefore expect it to predict less asymmetry than that of Yanson *et al.* The numerically computed curve for $a = 1$ Å, $l = 15$ Å, and $U = 2$ eV for our theory is the upper solid curve in Fig. 3. This curve, since it is a ratio of intensities, is independent of the values chosen for Z, δ, and ϵ. It is somewhat below the experimental points, as might be expected, since our square barrier potential does not allow for the asymmetry of the barrier-penetration probability, as demonstrated by the asymmetry of the elastic conductance vs voltage curves. Presumably a

more sophisticated model for the barrier potential, which included the interaction of the electrons with its own images and the unequal potential barrier heights for Pb and Al, could be constructed to fit the elastic current-voltage curve asymmetry. Any such model would push the theoretical curve up since the asymmetry of the elastic current-voltage curve opposes that of the inelastic intensities. Such a sophisticated model would be difficult to incorporate into our theory. An easy, though only approximate, correction is to multiply the ratio of the inelastic intensities by the ratio of the measured elastic conductances at each voltage. This correction results in the dashed curve of Fig. 3, which fits the experimental points well. Note that this barrier asymmetry correction is too small to help the theory of Yanson *et al.* appreciably.

C. Orientation selection rules

The theory of Scalapino and Marcus predicted that there should be no IETS intensity for a vibrational mode which resulted in an oscillating dipole moment parallel to the metal surface. This orientation rule is weakened slightly by off-axis scattering. Although the barrier penetration probability falls off rapidly for electrons scattered off the $\hat{z}$ axis, the initial and final volumes of phase space they can scatter into becomes larger for larger scattering angles. To estimate the relative importance of off-axis scattering, we calculated the integrand $G(\epsilon_F, \epsilon_F - eV, \Theta, \Theta', \varphi, \varphi')$ of Eq. (14) for a charge oscillating in the $\hat{z}$ direction, with $a = 1$ Å, $l = 15$ Å, $eV = 200$ meV, and setting $\Theta = \psi = \psi' = 0$. The quantity $2\pi \sin\Theta' G(\Theta')$, which is a measure of the relative contribution to the total IETS intensity due to scattering into one off-axis angle, when plotted against scattering angle Θ', peaks at ~4° and has a weighted average

$$\int_0^\pi d(\cos\Theta')\Theta' G(\Theta') \Big/ \int_0^\pi d(\cos\Theta') G(\Theta')$$

of ~7°. It is therefore important to consider scattering in three dimensions.

A numerical calculation based upon Eq. (14) for $U - \epsilon_F = 2$ eV, $l = 15$ Å, and $a = 1$ Å for the hydroxyl ion predicts that the IETS intensity for the O-H stretch mode should be 8.8 times stronger when the molecule is oriented perpendicular to the metal surface than when it is oriented parallel to the metal surface. A similar calculation for the infrared mode of CO_2 predicts that the ratio of the intensities for the two orientations should be 16.4. Therefore, while our theory predicts a weakening of the selection rule, it is still quite strong.

Experimental support for the presence of this selection rule exists in the tunneling spectrum of benzoic acid on alumina. Benzoic acid, which has a COOH acid group attached to a benzene ring, has had its tunneling spectrum carefully analyzed.[3,17] The agreement in vibrational-mode energies, between tunneling and optical studies, after proper correction of the tunneling data for the effects of superconductivity is made, is good to within a few tenths of a percent for most vibrational modes. The small discrepancies between tunneling and optical measurements can be attributed to the effect of the top metal electrode.[3]

However, as can be seen in the comparison between infrared and tunneling spectra shown in Fig. 4, there is one band at 1560 cm^{-1} in the infrared, which is markedly smaller in the tunneling spectrum. This mode is attributed to the antisymmetric stretch mode of the carboxylate group. Careful studies of the vibrational-mode frequencies of this group[18] show that it loses its hydrogen in chemisorbing, and that the two oxygens in the group are in equivalent sites: that they are equidistant from the oxide surface.

The resultant COO^- group has a symmetric and

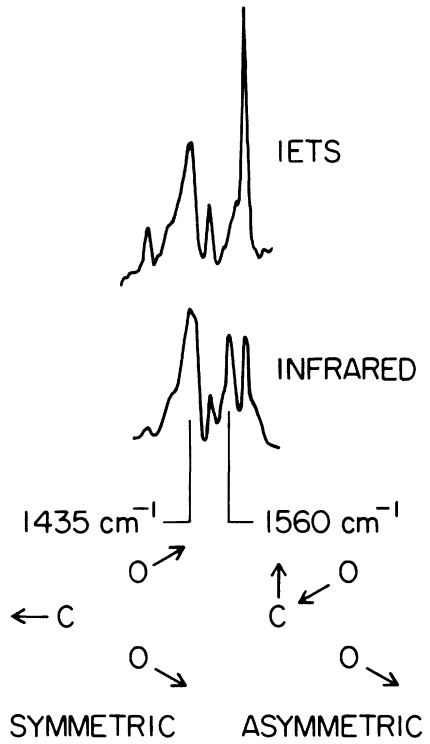

FIG. 4. Comparison of the tunneling vs infrared spectra of benzoic acid on alumina. Note the missing peak in the tunneling spectra at 1560 cm^{-1}. We believe that this peak is greatly reduced in intensity because of the orientation of the molecule on the surface, as predicted by our theory.

antisymmetric vibrational mode. These modes have their oscillating dipole moments at right angles to each other. Based on the above assignment of orientation, the symmetric mode has its oscillating dipole moment perpendicular to the oxide surface while the asymmetric mode has its oscillating dipole moment parallel to the oxide surface. Thus we would expect that the asymmetric mode would be much lower in intensity than the symmetric mode. Figure 4 shows that this is found experimentally.

D. Other selection rules

Observable vibrational modes in infrared spectroscopy involve an oscillation of the net dipole moment of the molecule. Observable modes in Raman spectroscopy involve an oscillation of the polarizability of the molecule. Tunneling spectra of anthracene indicate that both infrared and Raman modes are observed with comparable intensities.[17] However, calculations of Jaklevic and Lambe[1] indicate that the Raman modes should have roughly an order of magnitude smaller intensities than the infrared modes. The theory presented in this paper, in contrast, predicts that even with no polarizability accounted for, the Raman mode intensities should be nearly the same size as the infrared mode intensities. Further, it predicts that modes forbidden to both Raman and infrared spectroscopies should be observable with tunneling.

The reason for the breaking of the selection rules is as follows. In the matrix elements $M_{KK'_j}$, Eq. (9), terms like $e^{i\alpha_x b}$, $e^{i\alpha_y c}$, $e^{\alpha_\perp a}$ occur, where a, b, c are the displacement from the origin of the atom in the z, x, and y directions, and α_x, α_y, $\alpha_\perp$ are the momentum transfers parallel to the metal surface of a given scattering event. The matrix elements are spatially inhomogeneous because of these terms. The spatial inhomogeniety of the matrix elements causes the breaking of the selection rules.

This point can be made clear by an example. Consider the Raman vs ir stretching modes of CO_2, assumed to lie with its major axis in the $\hat{x}$ direction. In the ir mode the two oxygen atoms move in phase, the Z's and δ's for the oxygens have the same sign (the carbon atom has $Z=0$), and the matrix element is proportional to $e^{i\alpha_x b} + e^{-i\alpha_x b} = 2\cos\alpha_x b$, where b is the C-O bond length. For the Raman mode the oxygens move out of phase so the δ's have opposite signs. The matrix element in this case is proportional to $e^{i\alpha_x b} - e^{-i\alpha_x b} = 2i\sin\alpha_x b$. Even though the Raman mode has no net dipole moment, it has a finite matrix element for $\alpha_x \neq 0$. Numerical calculations, taking into account the different frequencies of the two modes, predict that the ir mode intensity of CO_2 should only be 20% larger than the Raman mode intensity if the molecule is oriented parallel to the metal surface. If the molecule is oriented perpendicular to the metal surface, the ir mode should be 4.2 times as intense as the Raman mode.

Two general comments should be made at this point. The first is that the breaking of the selection rules arises from the spatial inhomogeneity of the matrix elements, which in turn arises from off-axis scattering which some previous theories did not include. The second is that we expect selection rules to be less important for larger molecules, since the relevant parameter is the perpendicular momentum transfer times the spatial extent of the molecule. Thus we would expect that the infrared vs Raman selection rules would be even weaker for a larger molecule, like anthracene, as is observed experimentally.[17]

We conclude this section by discussing the observability of modes that are forbidden to both infrared and Raman spectroscopy. Molecules that have such modes tend to be complex, with the consequent difficulties of calculation and ambiguities in assigning Z's and δ's to a given normal mode. We choose, therefore, a simple, hypothetical linear four-atom chain molecule with an interatomic spacing of 1.54 Å (typical of C-C single bonds). A normal mode vibration of this molecule which is forbidden to infrared and Raman spectroscopies has displacements perpendicular to the axis of the molecule with atoms 1 and 3 in phase with each other and out of phase with atoms 2 and 4. If we take $Z=0.1$, $\delta=0.07$ Å, $l=15$ Å, $a=1$ Å, $U=2$ eV, $\epsilon=3$, $n=6\times10^{14}/\text{cm}^2$,[19] and assume that the molecule is oriented with its major axis parallel to the metal surface, we predict a change in conductance due to this mode of 0.16%, which would be readily observable. To our knowledge, no such forbidden mode has yet been identified experimentally.

IV. CONCLUSION

We have incorporated a new tunneling electron-vibrating molecule interaction potential into a transfer-Hamiltonian formalism for inelastic tunneling in metal-oxide-metal junctions. We have used the theory to calculate (i) absolute intensities, (ii) ratios of intensities for opposite bias polarities, (iii) ratios of intensities for different orientations, and (iv) ratios of intensities for Raman versus ir modes. The predictions agree qualitatively with experiment. Further, we predicted that vibrational modes forbidden to optical spectroscopies may be observable using electron tunneling.

Since the number of terms that must be considered increases only linearly with the number of atoms in a molecule, the theory can be used for complex molecules.

Although the results obtained above used values for Z, δ, and a that were taken from independent experimental measurements, there is the possibility of using a multiparameter fit to the intensities in inelastic electron tunneling to obtain values for effective Z's and δ's (as is now done in analyzing infrared spectra).[21]

We should finally remark that the interaction used above [Eq. (5)] does not take into account the polarizability of the molecule. The extra interaction due to the polarizability may be large enough to be important and should be calculated. The coupling to Raman-active modes described in this work is due to the local nature of the (Coulomb) interaction only.

ACKNOWLEDGMENTS

We wish to thank Professor D. Cannell, Professor J. Helman, Professor T. Holstein, Professor Y. Imry, Professor J. Klein, Professor D. Mills, and Professor H. Weinberg for valuable comments and suggestions. Special thanks go to D. Mills for bringing to our attention the close relationship of inelastic electron tunneling to the problem of inelastic scattering of slow electrons from surfaces.[20] Finally, we acknowledge the assistance of K. Kirtley in the numerical integrations.

---

*Work supported by the National Science Foundation.

†Present address: Dept. of Physics and Laboratory for Research on the Structure of Matter, University of Pennsylvania, Philadelphia, Pa. 19174.

[1]The first work in the field was done by R. C. Jaklevic and J. Lambe, Phys. Rev. Lett. 17, 1139 (1967); J. Lambe, and R. C. Jaklevic, Phys. Rev. 165, 821 (1968). A recent survey is contained in Ref. 2.

[2]P. K. Hansma, *Proceedings of the Fourteenth International Conference on Low Temperature Physics, Otaniemi, Finland*, 1975 (North-Holland, Amsterdam, 1975), p. 264.

[3]J. Kirtley and P. K. Hansma, Phys. Rev. B 13, 2910 (1976).

[4]D. J. Scalapino and S. M. Marcus, Phys. Rev. Lett. 18, 459 (1967).

[5]C. B. Duke, *Tunneling in Solids* (Academic, New York, 1969), Sec. 22d.

[6]J. W. Gadzuk, J. Appl. Phys. 41, 286 (1970).

[7]J. Klein, A. Léger, M. Belin, D. Défourneau, and M. J. L. Sangster, Phys. Rev. B 7, 2336 (1973).

[8]L. C. Davis, Phys. Rev. B 2, 1714 (1970); C. B. Duke, G. G. Kleiman, and T. E. Stakelon, *ibid.* 6, 2389 (1972); C. Caroli, R. Combescot, P. Nozières, and D. Saint-James, J. Phys. C 5, 21 (1972); T. E. Feuchtwang, Phys. Rev. B 10, 4121 (1974); 10, 4135 (1974); 13, 517 (1976).

[9]J. Bardeen, Phys. Rev. Lett. 6, 57 (1961).

[10]D. M. Newns, J. Chem. Phys. 50, 4572 (1969).

[11]N. D. Lang and W. Kohn, Phys. Rev. B 7, 3541 (1973).

[12]P. E. Cade, J. Chem. Phys. 17, 2390 (1967).

[13]J. B. Peri, J. Phys. Chem. 69, 211 (1965).

[14]P. W. Kruse, L. D. McGlauchlen, and R. B. McGuistan, *Elements of Infrared Technology* (Wiley, New York, 1963), p. 140.

[15]J. R. Kirtley and P. K. Hansma, Phys. Rev. B. 12, 531 (1975).

[16]I. K. Yanson, N. I. Bogatina, B. I. Verkin, and O. I. Shklyarevski Zh. Eksp. Teor. Fiz. 62, 1023 (1972) [Sov. Phys.-JETP 35, 540 (1972)].

[17]M. G. Simonsen, R. V. Coleman, and P. K. Hansma, J. Chem. Phys. 61, 3789 (1974).

[18]Y. Skarlatos, R. C. Barker, G. L. Haller, and A. Yelon, Surf. Sci. 43, 353 (1974).

[19]J. D. Langan and P. K. Hansma, Surf. Sci. 52, 211 (1975).

[20]E. Evans and D. L. Mills, Phys. Rev. B 5, 4126 (1972).

[21]See, for example, D. Steele, *Theory of Vibrational Spectroscopy* (Saunders, Philadelphia, 1971), Chap. 8.